ELSEVIER Science Press

Trans. Nonferrous Met. Soc. China 19(2009) s762−s766

Transactions of Nonferrous Metals Society of China

www.tnmsc.cn

Indentation size effect in microhardness measurements of $Hg_{1-x}Mn_xTe$

WANG Ze-wen(王泽温)[1, 2, 3], JIE Wan-qi(介万奇)[2], WANG Xiao-qin(汪晓琴)[4]

1. School of Materials Science and Engineering, Xi'an University of Technology, Xi'an 710048, China;
2. School of Materials Science and Engineering, Northwestern Polytechnical University, Xi'an 710072, China;
3. Department of Electronic Engineering, Tsinghua University, Beijing 100084, China;
4. College of Chemistry and Chemical Engineering, Shaanxi University of Science and Technology, Xi'an 710054, China

Received 10 August 2009; accepted 15 September 2009

Abstract: The effect of surface damaged layer and Te enrichment layer of $Hg_{1-x}Mn_xTe$ on the indentation size were studied experimentally. Based on the results, the indentation size effect (ISE) of $Hg_{1-x}Mn_xTe$ were discussed using different models, including Meyer's law, the power-law, Hays-Kendall approach and the theory of strain gradient plasticity. The results show that surface damaged layer weakens ISE of the wafers, but the Te enrichment layer reinforces it. The minimum test load necessary to initiate plastic deformation for different $Hg_{1-x}Mn_xTe$ wafers increases from 3.11 to 4.41 g with the increase of x from 0.05 to 0.11. The extrapolated surface hardness values of $Hg_{1-x}Mn_xTe$ are 347.21, 374.75, 378.28 and 391.51 MPa and the corresponding shear strength values are 694.53, 749.50, 756.56 and 783.12 MPa for $Hg_{1-x}Mn_xTe$ with the x values of 0.05, 0.07, 0.09 and 0.11, respectively.
Key words: $Hg_{1-x}Mn_xTe$; indentation size effect; microhardness

1 Introduction

Indentation hardness testing is widely used to express the mechanical properties of materials by variant researchers[1−5], especially when it is difficult to perform other mechanical tests. However, the mechanical and physical principles involved in the methods are still not well understood. The most intriguing phenomenon is the indentation size effect (ISE)[2−8] for which there is an increase in hardness with the decrease of indentation size (or load), as shown in Fig.1. The apparent hardness is a function of the applied load at low indentation test loads. However, it tends to be constant at high loads. For a long time, ISE has been considered a possible artifact caused by measurement errors or surface preparation problems. Recently, ILZE and JANIS[2] studied ISE of single crystals, polycrystals and amorphous solids etc. It was found that ISE is a popular phenomenon existing in single crystals, but is absent in fine-grained polycrystals. A size-dependent hardness of amorphous solids was observed only in the sub-micrometer surface layer. Therefore, ISE was considered an intrinsic property of the surface[2]. By a deep understanding of ISE, they suggested that the surface hardness and shear strength of materials could be deduced from microhardness.

A surface damaged layer nearly always exists on $Hg_{1-x}Mn_xTe$ wafer surface after the processing, such as cutting or polishing. Usually, 2%−5% Br-MeOH solution is used to remove the layer to obtain a clean surface, which will in return produce Te enrichment there[9]. The Te enrichment will interconnect with the surface damaged layer, which will make the problem more complicated.

The aim of this study is to determine ISE of $Hg_{1-x}Mn_xTe$, to reveal the effect of surface treatment methods on ISE. The surface hardness and shear strength of $Hg_{1-x}Mn_xTe$ will be estimated by measuring microhardness.

2 Experimental

2.1 Sample preparation

$Hg_{1-x}Mn_xTe$ wafers with 15 mm in diameter and 1.5 mm in thickness were cut from ingots perpendicular to

Foundation item: Project(50872111) supported by the National Natural Science Foundation of China
Corresponding author: WANG Ze-wen; Tel: +86-29-82312154; E-mail: wzwen@tsinghua.edu.cn

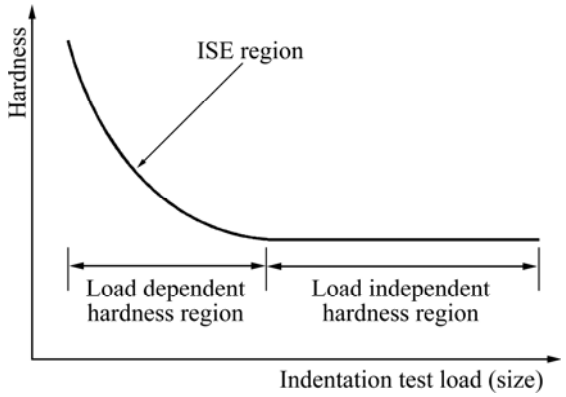

Fig.1 Schematic diagram of indentation size effect[2−8]

the centerline. The ingots were grown by the modified Vertical Bridgman Method. The wafers were first roughly polished by using diamond paste, and then finely polished using 5 and 0.5 μm MgO powder until there is no any visible nick on the surface. Finally, the wafers were chemically etched in 2%(volume fraction) Br-MeOH solution to remove surface damaged layer. The composition of the wafer was measured using electron probe.

2.2 Sample measurements

Hardness measurements were performed at room temperature by Vickers hardness tester attached to a Leica metallurgical microscope. The art closed loop load cell technology was used to measure the applied force, ensuring the loading force to be constant during the test dwell time. The Vickers indenter is a diamond square-based pyramid with an angle of 136° between faces. The depth of the indentation is about one-seventh of its diagonal length. The applied indentation loads were 25, 50, 100 and 200 g, respectively. The indenter was kept in contact with the surface for 15 s for all the trials. Six measurements were carried out at different sites on the middle of each wafer, and the average values were taken as the hardness of the wafers. The distance between two indentation points was three times more than the pit diagonal length to avoid any mutual influence of the indentations.

The microhardness measured by Vickers method is defined as the ratio of the load applied to the projected area of the indentation and is expressed by the following relation[10]:

$$H_{\mathrm{V}} = 1.854\left(\frac{P}{d^2}\right) \tag{1}$$

where H_{V} is the Vicker's microhardness; P is the applied load and d is the diagonal length of the impression in mm.

3 Results and discussion

Fig.2 shows the variation of microhardness (H_{V}) with the applied load (P) for $Hg_{0.94}Mn_{0.06}Te$ with polished and etched surface. It is seen that H_{V} values of the wafers after etching for 3 min and 5 min follows ISE relation shown in Fig.1. But before etching, H_{V} on the only polished surface almost keeps constant at the lower applied load from 25 to 200 g, and only have a small drop of hardness at the load of 200 g. When the sample surface is etched for 3 min and 5 min, H_{V} apparently increases with the increase of etching time for all the applied loads between 25 to 200 g. The investigations showed that the thickness of the surface damaged layer of $Hg_{1-x}Mn_xTe$ wafer surface after polishing was 15−17 μm[11−12]. Table 1 lists the variation of the thickness of the surface layer removed Δd through etching with the etching time, which were calculated using the following relation:

$$\Delta d = \frac{1}{2}\left(d_0 - \frac{m^*}{m_0} \times d_0\right) \tag{2}$$

where d_0 is the thickness of the wafer before etching; m_0 and m^* are the masses of the wafer before and after etching, respectively.

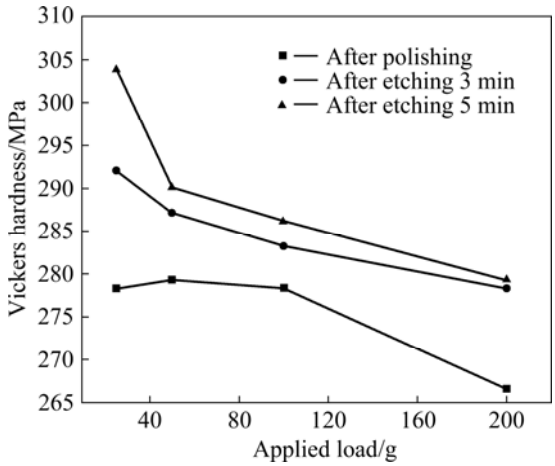

Fig.2 Dependence of Vickers hardness of $Hg_{0.94}Mn_{0.06}Te$ on applied load

It can be seen that after etching for 3 min, the surface damaged layer was fully removed. When the etching time was prolonged, an about 20 Å-thick Te enrichment layer was formed on the surface[9]. Because the surface damaged layer softens the surface, the hardness of non-etched surface does not increase following the normal ISE behavior at lower load. However, Te enrichment layer hardens the surface. Therefore, different from the non-etched surface, the over-etched surface with a Te enrichment layer shows a

Table 1 Mass and thickness of surface layer removed of $Hg_{0.94}Mn_{0.06}Te$ wafer after various etching time

Etching time/s	Mass/g	Thickness/mm	Thickness of surface layer removed/μm
0	1.712	1.196	0
30	1.701	1.188	4.0
60	1.693	1.183	6.5
120	1.679	1.173	11.5
180	1.666	1.164	16
240	1.655	1.156	20
300	1.643	1.148	24

higher hardness. It can be concluded that the surface damaged layer weakens ISE behavior of the $Hg_{0.94}Mn_{0.06}Te$ wafers, but that of the Te-rich layer reinforces it. The hardness measured on the $Hg_{0.94}Mn_{0.06}Te$ surface after 3 min etch is very close to that of a perfect $Hg_{0.94}Mn_{0.06}Te$ surface, and should be chosen for ISE researches.

3.1 Meyer's law

Fig.3 shows the variation of microhardness (H_V) of $Hg_{1-x}Mn_xTe$ with the applied load (P). It can be seen that H_V for all of the wafers keeps decreasing with the increase of the applied load from 25 N to 200 g. The critical indentation depth h_0 suggested by ILIE and JANIS[2] for $Hg_{1-x}Mn_xTe$ crystal is over 15 μm, beyond which H_V becomes independent of applied load. ISE of $Hg_{1-x}Mn_xTe$ based on the experimental results was analyzed with Meyer's law[2, 6, 10], which is widely used to explain ISE behavior. According to Meyer's law, the relationship between the applied load (P) and the indentation size (d) can be written as

$$P=kd^n \tag{3}$$

where the exponent n is the Meyer's index, and k is the standard hardness constant. The Meyer's index n is usually used as a measure of ISE. When $n<2$, the hardness decreases with the increase of applied load. The index n of $Hg_{1-x}Mn_xTe$ can be obtained from the plots of $\ln P$ against $\ln d$, as shown in Fig.4, and the fitted n values are listed in Table 2. It is seen that the index n decreases from 1.93 to 1.90 with the increase of x value from 0.05 to 0.11, meaning that ISE is more significant for $Hg_{1-x}Mn_xTe$ with higher x value. Because of the solid solution hardening effect of Mn^{2+}, the hardness of $Hg_{1-x}Mn_xTe$ increases with x as shown in Fig.3. Therefore, the results also show that ISE increases with the increase of material hardness.

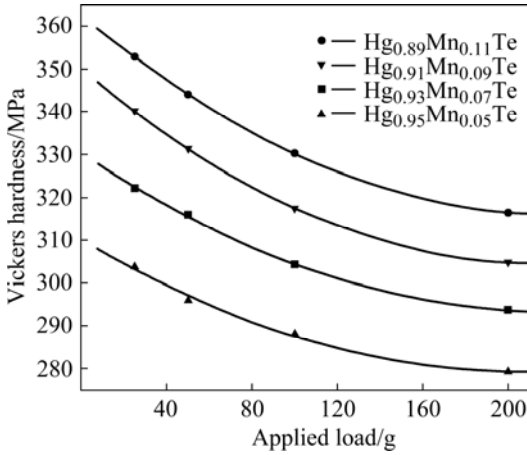

Fig.3 Dependence of Vicker's hardness of $Hg_{1-x}Mn_xTe$ on applied load

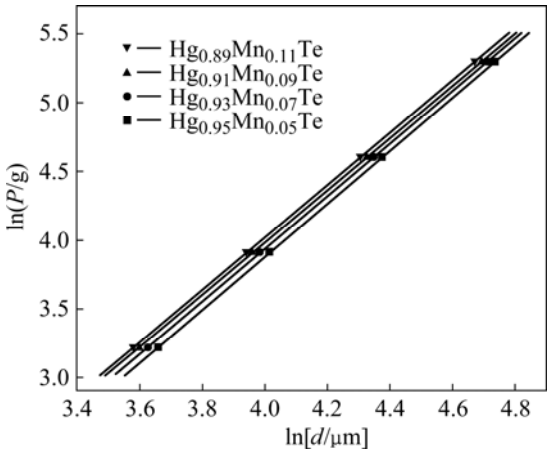

Fig.4 Plot of ln$P$ vs ln$d$ according to Meyer's law

3.2 Power law

Even though Meyer's law can explain ISE behavior of $Hg_{1-x}Mn_xTe$ qualitatively, the physical significances of the parameters k and n are still not well understood because it is just an empirical relationship, and is initially brought forth based on spherical indentations. For pyramidal indentation, a power-law relationship between the hardness H_V and the indentation depth h defined by Eq.(4) was confirmed by many experimental data[13]:

$$H_V=ch^{-m} \tag{4}$$

where c is a constant and m is the power-law exponent or the ISE index. According to Eq.(4), the plot of lgH_V vs. lg$h$ should yield a straight line. Fig.5 shows such plots, where the parameters c and m can easily be determined from the intersection point and the slope of the curves, respectively. The fitting results are shown in Table 2. m quantitatively characterizes ISE behaviors. Opposite to the Meyer's index n, m decreases from −0.078 to −0.100 with the increase of x from 0.05 to 0.11. According to the relationship of lgH_V vs lg$h$, the real surface hardness of materials can be obtained using extrapolating the lgH_V vs lg$h$ curves to the indentation depth equal to the lattice constant. Experimental data of many materials show that

Table 2 Fitting results of parameters n, m, P_m, k_1 and surface properties

Parameter	Meyer index, n	ISE index, m	P_m/g	k_1/MPa	Surface strength/MPa	Shear strength/MPa
$Hg_{0.95}Mn_{0.05}Te$	1.93	−0.078	3.11	148.96	347.21	694.53
$Hg_{0.93}Mn_{0.07}Te$	1.92	−0.087	3.70	155.82	374.75	749.50
$Hg_{0.91}Mn_{0.09}Te$	1.90	−0.10	4.24	161.70	378.28	756.56
$Hg_{0.89}Mn_{0.11}Te$	1.90	−0.10	4.41	167.58	391.51	783.12

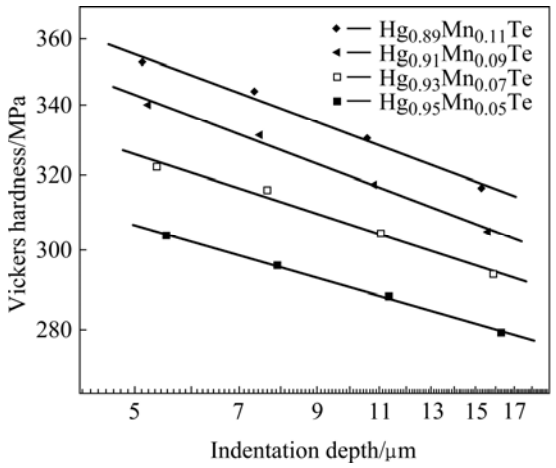

Fig.5 Dependence of hardness of $Hg_{1-x}Mn_xTe$ wafer surfaces on indentation depth

the extrapolated surface hardness values are about two times higher than the theoretical shear strength[2]. The extrapolated surface hardness and shear strength of $Hg_{1-x}Mn_xTe$ are listed in Table 2. It is seen that the surface hardnesses of $Hg_{1-x}Mn_xTe$ are 347.21, 374.75, 378.28 and 391.51 MPa, and corresponding shear strength values are 694.53, 749.50, 756.56 and 783.12 MPa, for $Hg_{1-x}Mn_xTe$ with the x values of 0.05, 0.07, 0.09 and 0.11, respectively.

3.3 Hays−Kendall approach

HAYS and KENDALL[14] assumed that the resistance to indentation deformation could be evaluated by considering it a Newtonian resistance pressure of the specimen itself. When a load P is applied to a specimen, P is partially affected by a small resistance pressure. Based on the hypothesis, P is described as[14]

$$P=P_m+k_1d^2 \tag{5}$$

where P_m is the minimum test load necessary to initiate plastic deformation, below which only elastic deformation occurs; k_1 is a load-independent constant. Fig.6 shows the plots of P vs d^2 according to Hays−Kendall approach. The data show an intimated linear relationship. This implies that the Hays−Kendall approach is suitable for describing the microindentation data of $Hg_{1-x}Mn_xTe$. The calculated P_m and k_1 from experimental data are listed in Table 2. It is seen that P_m increases from 3.11 to 4.41 g with the increase of x from 0.05 to 0.11. This means that the necessary minimum test load increases with the hardness of $Hg_{1-x}Mn_xTe$.

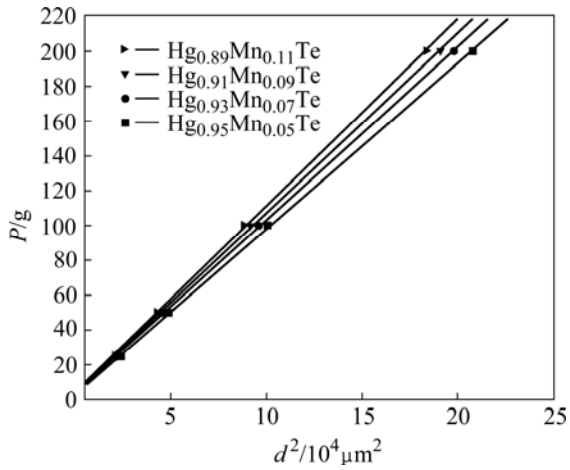

Fig.6 Plot of P vs d^2 according to HAYS and KENDALL approach

3.4 Theory of strain gradient plasticity

During the last decade, the mechanisms of ISE based on the theory of strain gradient plasticity (SGP) have been developed[15−16]. From the Taylor's theory of dislocation work hardening for crystalline materials, it was suggested that both the statistically stored dislocations created by a homogenous strain and geometrically necessary dislocations related to the strain gradients contribute to the hardness. ISE is related to the increasing contribution of geometrically necessary dislocations at small indentation depths. A simple model of geometrically necessary dislocations has been derived by STELMASHENKO et al[17]. Using this model, NIX and GAO[16] found that the strain gradient law implies the following relationship for the hardness:

$$\frac{H_V}{H_0}=\sqrt{1+\frac{h^*}{h}} \tag{6}$$

where H_0 is the hardness arisen from the statistically stored dislocations in the absence of strain gradient effects and h^* is the characteristic length (depth), at which the effect of strain gradient becomes comparable to that of strain. Fig.7 shows that there exists remarkable

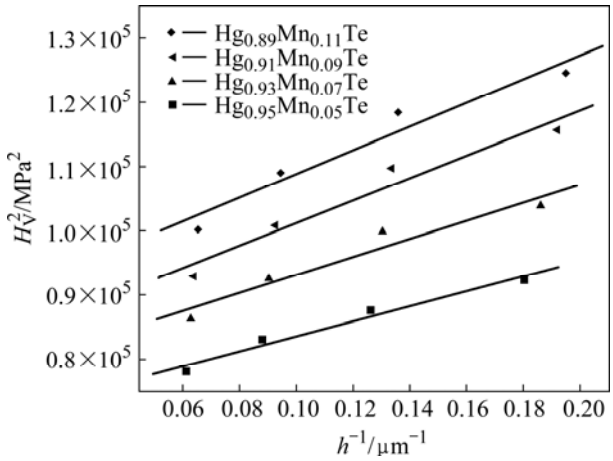

Fig.7 Plot of H_V^2 vs h^{-1} according to theory of strain gradient plasticity

deviation between the experimental data and the fitting lines of H_V^2 vs $1/h$. This indicates that SGP model as a simplified approach is insufficient for the description of such a complex phenomenon of ISE.

Based on the above discussion, we can conclude that the power-law relationship between the hardness and the indentation depth and the Hays–Kendall approach are more preferable in this work. They are not only valid for the description of ISE of $Hg_{1-x}Mn_xTe$ but also provide an estimation of the surface hardness, shear strength and the minimum load required for initiating the permanent deformation. However, the Meyer's law gives only limited information and SGP model is insufficient to describe ISE behavior of $Hg_{1-x}Mn_xTe$.

4 Conclusions

1) The surface damaged layer of $Hg_{1-x}Mn_xTe$ wafers produced by polishing weakens the indentation size effect, but Te enrichment on the wafer surface due to over-etching reinforces it.

2) The minimum test loads necessary to initiate plastic deformation for $Hg_{1-x}Mn_xTe$ increases with the x value, which are determined to be 3.11, 3.70, 4.24 and 4.41 g for $Hg_{1-x}Mn_xTe$ with the x values of 0.05, 0.07, 0.09 and 0.11, respectively.

3) The surface hardness values of $Hg_{1-x}Mn_xTe$ are 347.21, 374.75, 378.28 and 391.51 MPa, and corresponding shear strength values are 694.53, 749.50, 756.56 and 783.12 MPa, for $Hg_{1-x}Mn_xTe$ with the x values of 0.05, 0.07, 0.09 and 0.11, respectively.

4) The power-law relationship between the hardness and the indentation depth and the Hays–Kendall approach are more preferable to explain ISE of $Hg_{1-x}Mn_xTe$, by which the surface hardness, shear strength and the minimum load required for initiating the permanent deformation of $Hg_{1-x}Mn_xTe$ can be also estimated.

References

[1] SUSHANTA K K, SAMANTARAY B K, BASU S. Effect of Ni concentrations on the microhardness of GaNiSb ternary alloys [J]. J Alloys Compd, 2006, 414: 235−239.

[2] ILZE M, JANIS M. Size effects in micro- and nanoscale indentation [J]. Acta Mater, 2006, 54: 2049−2056.

[3] QIAN J, DAEMEN L L, ZHAO Y. Hardness and fracture toughness of moissanite [J]. Diamond Relat Mater, 2005, 14: 1669−1672.

[4] KOUBAITI S, COUDERC J J, LEVADE C, VANDERSCHAEVE G. Photoplastic effect and Vickers microhardness in III–V and II–VI semiconductor compounds [J]. Meas Sci Technol A, 1997, 234/236: 865−868.

[5] SANGWAL K, SUROWSKA B, BLAZIAK P. Relationship between indentation size effect and material properties in the micro-hardness measurement of some cobalt-based alloys [J]. Mater Chem Phys, 2003, 80: 428−437.

[6] SHARMA B L. Anisotropic lamellae growth and hardness of eutectic composite alloy Pb-Sn [J]. J Alloys Compd, 2004, 385: 74−85.

[7] TUCK J R, KORSUNSKY A M, DAVIDSON R I, BULL S J, ELLIOTT D M. Modelling of the hardness of electroplated nickel coatings on copper substrates [J]. Surf Coat Technol, 2000, 127: 1−8.

[8] WELLMAN R G, TOURMENTE H, IMPEY S, NICHOLLS J R. Nano and microhardness testing of aged EB PVD TBCs [J]. Surf Coat Technol, 2004, 188/189: 79−84.

[9] ROUSE A A, SZELES C, NDAP J O, SOLDNER S A, GASPAR D J, ENGELHARD M H, LEA A S, SHUTTHANANDAN V, THEVUTHASAN S. Interfacial chemistry and the performance of bromine-etched CdZnTe radiation detector devices [J]. IEEE Trans Nucl Sci, 2002, 49: 2005−2009.

[10] KÖLEMEN U, UZUN O, YILMAZLAR M, GÜÇLÜN, YANMAZ E. Hardness and microstructural analysis of $Bi_{1.6}Pb_{0.4}Sr_2Ca_{2-x}Sm_xCu_3O_y$ polycrystalline superconductors [J]. J Alloys Compd, 2006, 415: 300−306.

[11] YAMAGUCHI N, WATANABE J. Evaluation of process damage depth using dislocation-free GaAs wafers [J]. J Electrochem Soc, 1990, 137: 2849−2853.

[12] CHEN Jian-bang, QIAN Jia-yu, YANG Jun. Observation of damage layer on surface of GaAs wafer by TEM [J]. Chinese Journal of Rare Metals, 1998, 22(5): 392−395.

[13] MOTT B W. Micro-indentation testing [M]. London: Butterworths, 1956.

[14] HAYS C, KENDALL E G. An analysis of knoop microhardness [J]. Metall, 1973, 6: 275−282.

[15] GERBERICH W W, TYMIAK N I, GRUNLAN J C, HORSTEMEYER M F, BASKES M I. Interpretations of indentation size effects [J]. J App Mech, 2002, 69: 433−442.

[16] NIX W D, GAO H. Indentation size effects in crystalline materials: A law for strain gradient plasticity [J]. J Mech Phys Solids, 1998, 46: 411−425.

[17] STELMASHENKO N A, WALLS M G, BROWN L M, MILMAN Y V. Microindentations on W and Mo oriented single crystals: An STM study [J]. Acta Metall Mater, 1993, 41: 2855−2865.

(Edited by YANG Hua)